Spatial and temporal variations in sediment accumulation rates in a freshwater tidal marsh channel of the Patuxent River, Maryland

Kelsey Lynn Wood

Advisors: Karen Prestegaard
Alan J. Kaufman

GEOL 394

2015

Abstract

Sea level is rising at a rate of 2 to 4 millimeters a year in the Chesapeake Bay region, causing concern for the survival of tidal wetlands. The tidal marshes must adapt to the rising sea level in order to continue performing their key role in our ecosystem. The tidal channels will have to maintain a net accretion of sediment, either organic or mineral, in order to remain in equilibrium with the sea level. This study focuses on a freshwater tidal marsh channel network off of the Patuxent River near Upper Marlboro, Maryland ($38^{o}48'05''$ N and $76^{o}42'20''$ W). Through the measurement of channel cross sections and calculations of flow velocity, estimates were made for the transport, deposition, and erosion of sediments in this channel. Fifty centimeter deep cores were retrieved from various locations along the channel and analyzed to determine their sedimentary and geochemical characteristics. Clear spatial trends include a decrease in bulk density and an increase in organic matter with increased distance from the channel inlet. The cores are also analyzed for ^{15}N, ^{13}C, and ^{34}S abundances revealing significant down core trends believed to be the result of environmental changes related to land use of the drainage basin and the construction of a dam upstream in the Patuxent River. The coupled stratigraphic geochemical shifts were used as time constraints in order to approximate relative depositional rates in the tidal marsh channel. It appears as though the marsh is keeping pace with sea level rise with an estimated accumulation rate of 2.7 millimeters a year. It is however evident that different sediment types behave differently within the channel, with observations of seasonal organic matter erosion.

Table of Contents

Statement of the problem

Freshwater tidal marshes are an important part of coastal ecosystems. They act as buffers for storm surges, habitats for aquatic life, and have ample economic value. (Mitsch & Gosselink, 2000) They are vital to the state of water chemistry as they are centers of sediment retention and denitrification (Seldomridge & Prestegaard, 2014). Marshes ability to store nutrients becomes ever more vital to the health of an estuary with an increase of urban and agricultural land use within the basin. It is of great concern as to whether tidal marshes will be able to adapt to the changing environment. Sea level has been consistently rising at the present rate of ~3 mm/yr for more than 350 years. (Kearney & Stevenson, 1991) In order for marshes to adapt, net sediment accumulation should be equal to the local apparent rise in sea level. Many factors affect the accumulation of sediment within a tidal channel network, such as sediment concentrations within the estuary, channel form, water velocities, and the presence of vegetation within the channel. To maintain equilibrium, net accumulation has to occur in the channel as well as on marsh surfaces. Channel environments, however, are considerably more erosive than marsh platforms. In particular, organic sediment may be seasonally exposed to erosion during the cold season when die-back of aquatic vegetation exposes surfaces to erosive forces. In order to have a net gain in sediment accumulation and thus marsh elevation, the net gain will have to exceed the sum of the net loss and sea level rise. Net gain includes the deposition of mineral sediment, and the accumulation of biomass and organic sediment. Net loss includes compaction, decomposition of organic materials, and erosion. Sediment loads in the estuary will have to be sufficient to maintain elevation, and with increased sea level rise rates it is necessary to have an increase in sediment concentration. (Tambroni & Seminara, 2012) The climate is also of great influence on marsh elevation because of the immense effect vegetation has of flow resistance and sediment trapping. In freshwater tidal marshes each plant species has a specific depth range of habitat and stem density, creating spatial variation in sediment trapping during the growing season. (Statkiewicz, 2014) Vegetation can also concentrate the flow to lesser vegetated areas increasing the relief of channel of the form by increasing erosion on non-vegetated areas and accumulating sediment in vegetated areas. (Temmerman, Bouma, Koppel, Wal, Vries, & J.Herman, 2007)

Previous Work

Initial sediment accumulation depends on sediment availability and flow velocity of water in tidal channels. Incoming sediment supply, and channel hydraulics (flow velocity and shear velocity) will determine the range of sediment types and sizes that can be transported, deposited, and entrained under various conditions in tidal channels. For example, mineral sediment cannot be transported to upstream reaches of a channel if flow is insufficient to carry the particles in suspension or if the transport velocity is unable to carry particles any significant distance during a tidal cycle. Mineral sediment deposition rates are significantly higher along levees and other locations where sand and other large particle sizes can be transported and deposited, therefore, the maximum size of sediment that can be transported within a channel is an important factor in both deposition and erosion processes.

The maximum suspended particle size and its vertical distribution within the water column can be predicted based on channel morphology, and tidal hydrodynamics. Rouse (1937) developed a theory for the vertical distribution of sediment, which is based on the vertical velocity profile in a channel cross section and the fall velocity of the sediment. Suspension occurs when upwards turbulence (the vertical component of velocity) is greater than the fall velocity of the particle, W_s. Particles with high fall velocities will tend to be transported near the bed. Previous studies have indicated that the turbulent intensity is proportional to the shear velocity, u*, which can be calculated as:

$$u^* = \sqrt{gdS} \quad (1)$$

Where *g* is gravitational acceleration, *d* is flow depth, and *S* is gradient.

The fall velocity can be calculated as:

$$W_s = \frac{RgD^2}{C_1 v + (0.75 C_2 RgD^3)^{(0.5)}} \quad (2)$$

Where *Rg* is the particle Reynolds number, *D* is the grain diameter, *v* is the kinematic viscosity of the matrix which is in this case is water, and C_1 and C_2 are coefficients that depend upon grain size and shape. (Ferguson and Church, 2006).

The vertical distribution of sediment in the water column is calculated using the Rouse equation, where the vertical distribution of sediment of each grain size is governed by the exponent, *P*:

$$P = \frac{W_s}{\beta k u_*} \quad (3)$$

Where β is assumed to be 1.0, and k is Von Karman's constant (0.4).

Rouse's equation to determine the sediment concentration relative to the sediment concentration near the bed, *C/Ca*, for any given depth can be calculated:

$$\frac{C}{C_a} = \left(\frac{d-y}{y} * \frac{a}{d-a}\right)^Z \quad (4)$$

Where C is concentration, d is total depth, y is the distance above the bed, and a is an arbitrary distance above the bed used as a reference level (usually taken to be 0.05 of the depth above the bed).

The Rouse equation can be used to evaluate the distance above the bed that sediment can be transported in suspension and thus whether sand or silt sized sediment can be transported out of the main channel and onto marsh platforms at various elevations.

The distance that particles can be carried in suspension into tidal channels is dependent upon the velocity (velocity=distance*time). Velocity in tidal channels can be spatially and temporally variable because it depends on the depth and morphology of the channel as well as the presence or absence of vegetation growing within the channel. Submerged vegetation can interact with water flow in various ways. Flow through and around flexible canopies can create progressive waves along the canopy surface called *monami*. This interaction creates an upper layer of turbulence and higher velocities, and a lower layer of slow velocities within the vegetation. (Neph & Ghisalberti, 2008). This variation in velocities was also observed by Leonard and Luther (1995) in a salt water marsh in Florida (Fig. 1).

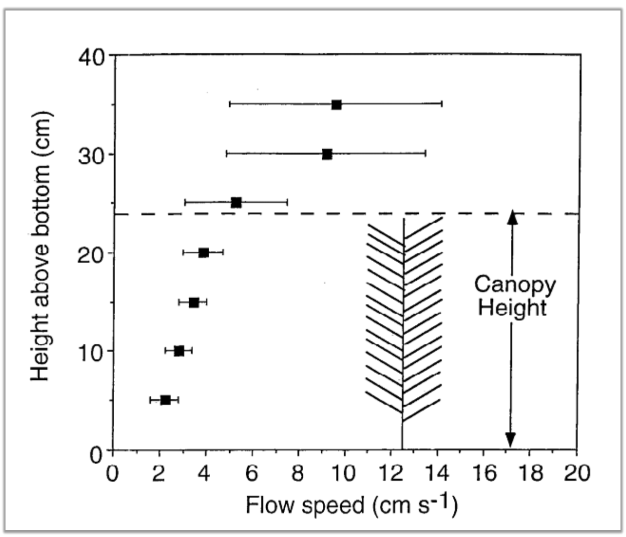

Figure 1: Velocity measurements in a saltwater tidal marsh by Leonard and Luther show a significant decrease in flow velocity in the vegetated area of the channel. (Leonard & Luther, 1995)

Freshwater tidal marshes tend to support a wider range of emergent and submerged plant species than salt marshes, and the emergent plant species tend to grow in a specific range of water depths within the channel creating distinct vegetative zones. (Statkiewicz, 2014). There are various species on the marsh platform, but species that grow within the channel are those that will effect channel sediment accumulation by attenuating flow rates. The predominant emergent species that grows in the Patuxent tidal channel chosen for this study is *Nuphar* (Fig. 2), which grows in a specific range of water depth between high and low tide water levels, and rarely grows at any depth greater than one meter below the marsh platform (Statkiewicz, 2014)

Figure 2: Nuphar growing in the marsh of study; picture is taken during low tide

The ability of water, sediment, and nutrients to flow into the tidal marsh channel will determine the sediment accumulation and denitrification capacity of a marsh. Variations in the hydrodynamics of a tidal system can produce an uneven distribution of new water introduced to various parts of the channel. Water drains from the tidal inlets on the outgoing tide and is replaced by new water with the next incoming tide. In the further reaches of the channel network, water draining out with an outgoing tide may be forced back into the channel by the next incoming tide. This is due to insufficient time between tides to entirely drain the upper reaches of the channel. This effect is increased during summer months when vegetative flow resistance is at a maximum, which decreases the flow velocity along with the transport of sediment and nutrients. This was observed in a previous study on a Patuxent fresh water tidal marsh (Fig. 3) by Jenner (2011).

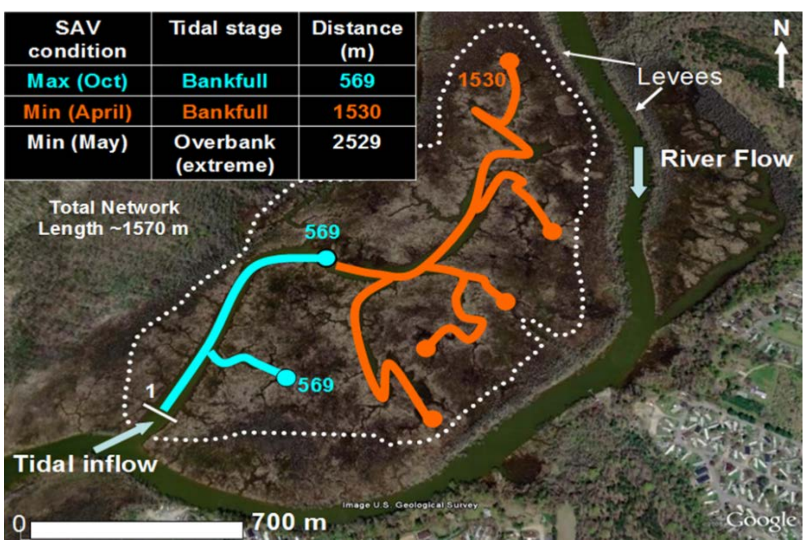

Figure 3: Distance of incoming water parcels at high tide during maximum (light blue) and minimum (red) vegetative seasons. Data suggest that new water is primarily distributed in the lower portion of the marsh system. (Jenner, 2011)

This study focuses on one fresh water tidal channel network on the upper Patuxent River Estuary, east of Upper Marlboro. The center of the marsh is about $38^0$48’05”N and $76^0$42’20”W (Fig. 4). Previous work has been done on this marsh and similar marshes by Maryland students Statkiewicz, (2014) and Fowler (2014). Their research focused on the relationship between vegetation type and channel morphology at different tidal inlets, including the marsh that I am examining for this study. Statkiewicz (2014) found that sediment accumulates and erodes over an annual cycle, although there is net accumulation of sediment that is keeping pace with sea level rise. Similar to this study, Fowler (2014) collected sediment cores focusing on multiple channel inlets, including the Nuphar-dominated channel network investigated here. The sediment core samples were analyzed for percent bulk organic matter, as well as carbon and nitrogen abundance and isotope compositions. At the inlet to the tidal marsh Fowler (2014) discovered a shift towards greater ^{15}N abundances in the core samples at a depth of about 30 cm.

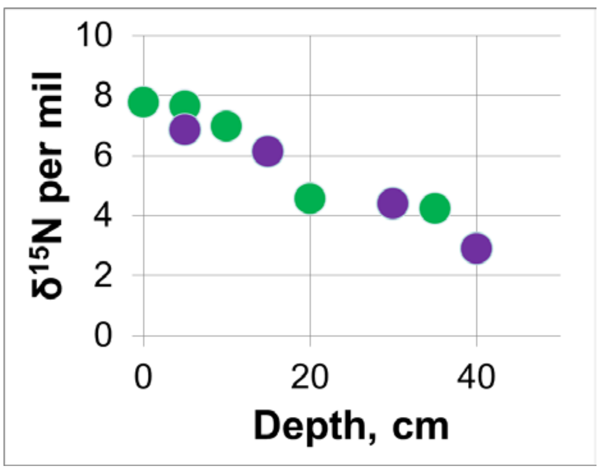

Figure 4: Plot of ^{15}N abundances found in the sediment cores taken from the Nuphar-dominated marsh inlet as a function of core depth by Fowler (2014).

The increase in ^{15}N observed through the upper portion of the core was interpreted to be the result of denitrification in the Patuxent River watershed after the 1950’s when nitrogen fertilizers became broadly accessible. This timing corresponds with overall elevated nitrogen levels observed in the Patuxent River (Boynton, et al., 2008). Fowler (2014) and Statkiewicz (2014) both analyzed sediment from the inlets to the channels. Due to the inlet’s proximity to the Patuxent River, nitrogen isotope compositions measured at these locations are likely representative of nitrogen levels in the Patuxent River.

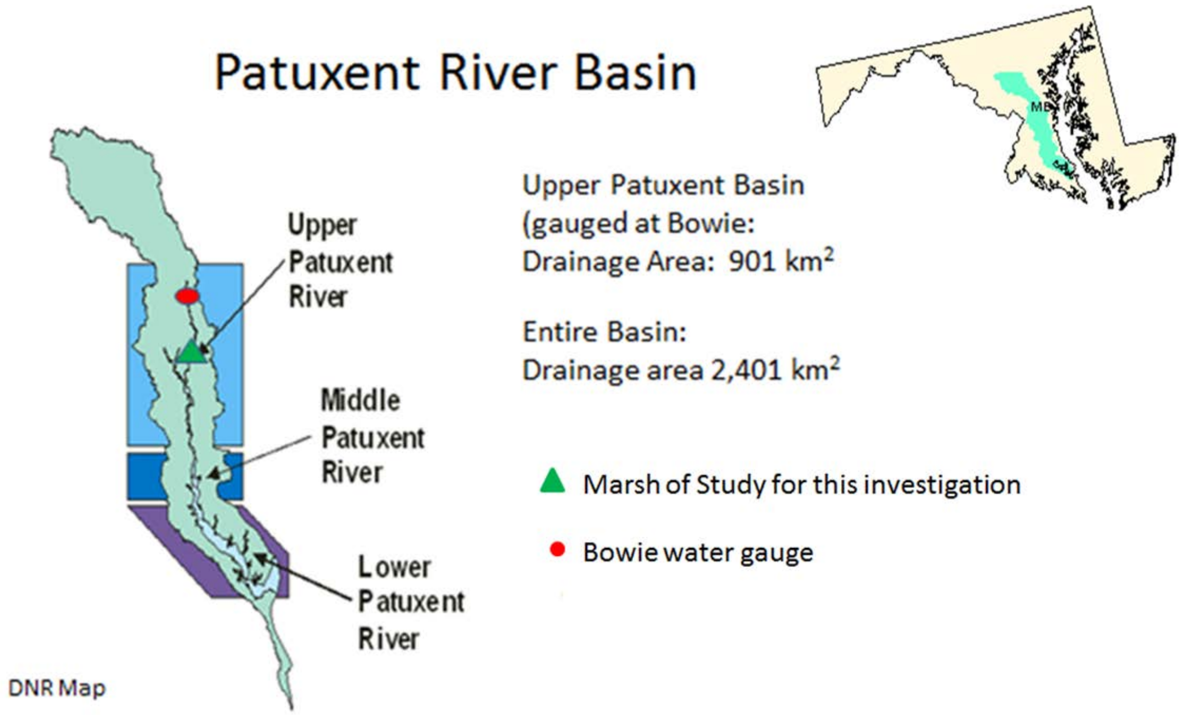

Figure 5: Map of the Patuxent River basin. Images modified from Maryland DNR

The Patuxent River basin is the largest wholly contained in the state of Maryland spanning a drainage area of 2401 km^2. Within the past 50-100 years the Patuxent has become eutrophic (rich in nitrates, phosphates, and organic nutrients) largely due to the 2-5 fold increases in nitrogen availability since 1970. (Fisher, HagyIII, Boynton, & Williams, 2006) The Patuxent watershed has gone from being primarily forested to become >15% urban and >20% agricultural. Agricultural runoff rich in fertilizer as well as urban sewage have significantly increased nutrient loads to the Patuxent. The Patuxent watershed has a high land to water ratio as compared to other Chesapeake Bay tributaries, so nutrient loads are more concentrated within the waterway. (Fisher et. al., 2006)

Nitrogen rich fertilizers, if formed by the industrial Haber process, have an isotopic composition equal to atmospheric nitrogen composition. Since the implementation of improved agricultural practices, residual nitrate that is not used by crops infiltrates into the soils and groundwater, eventually contributing to the streamflow in major tributaries to the Chesapeake bay. These longer and potentially anoxic groundwater flow paths allow for enhanced bacterial denitrification that would enrich the base flow in the heavier ^{15}N isotope by releasing ^{14}N to the atmosphere as N_2O or N_2: $H_2 + NO_3^- \rightarrow H_2O + N_2$.

In this study, I examine the spatial distributions of sediment type (organic versus mineral), and temporal events that are recorded in sediment cores. I am interested in whether the sediment cores retrieved in portions of the tidal channel upstream of the inlet record the same stratigraphic distributions of nitrogen isotopic composition observed in the inlet cores by previous workers.

Hypotheses

1. The proportion of mineral sediment to organic sediment will decrease with distance upstream into the tidal channel network.

    a. Core samples taken near the channel inlet will have the highest mineral sediment content and the highest bulk density.
    b. Core samples at upstream locations will have the highest organic sediment content and the lowest bulk density.

2. Although sediment type (organic or mineral) will vary spatially, the rate of accumulation is determined by accommodation space rather than sediment availability, and therefore will be similar throughout the tidal channel network. Consequently, the shift in ^{15}N composition observed in Fowler's (2014) cores, will occur at similar depths in cores taken from all locations.

Null Hypotheses

There will be no observed spatial variation in sediment composition throughout the channel network.

A shift in ^{15}N composition will be found at varying depths within the cores or not at all.

Study Site and Methods

Initial reconnaissance was done to locate a tidal marsh and refine the scope of the study. The study marsh was selected because: a) it is one of three large marshes in the upper Patuxent estuary that is accessible by kayak from the Route 4 boat landing; b) No major marsh tributaries are obstructed or altered. c) the tidal channels are partially covered by submerged aquatic plant *Nuphar* (Statkiewicz, 2014). The tidal channel network is located at approximately 38^{0}48'05"N and 76^{0}42'20"W, branching off of the east bank of

Figure 6: Marsh on which this study is focused. Upper Marlboro, Maryland. 38^{0}48'05"N and 76^{0}42'20"W

the Patuxent River. The east border of the marsh is constrained by a forested area. Across the Patuxent to the west and on the east of the forested area are agricultural lands. There are small urban centers in the surrounding area.

Channel morphology measurements

Channel morphology measurements were made from both air photos and from field measurements. Air photo imagery is available from USGS for multiple years through Google Earth. This platform was used to view the tidal channel network as a whole.   Measurements were made of total channel width, water width, and vegetated width at 20 m intervals along the channels. Measurements for summer conditions were performed on air photos from 8/28/2010. These data are plotted as a function of distance upstream.

Sites for field cross section measurements were selected to provide data for intervals along the main channels and at sites near distributary junctions. Each cross section site was marked in the field with two polyvinylchloride (pvc) pipes. Each pipe is anchored deep into the marsh and a reference level, including its elevation relative to the marsh platform, is marked on the pipe. Six cross sections were measured at permanently anchored sites during high tide. I also acquired data from a cross section near the inlet of the channel that was previously measured by Statkiewicz (2014). Sites were anchored by 0.5 in diameter pvc pipes 5 feet in length pushed 4 feet into the channel platform on direct opposite sides of the channel to be measured. A tape measure was attached to both poles, and depth was measured with a USGS style wading rod at 0.3 or 1.0 m intervals depending on the width of the channel. Corrections were made for any rise or fall in tide during the time we were measuring any one cross section. If a cross section was measured at a time other than high tide, the water level was used as a reference level and measurements were adjusted to the reference level marked on the pvc pipe anchor.

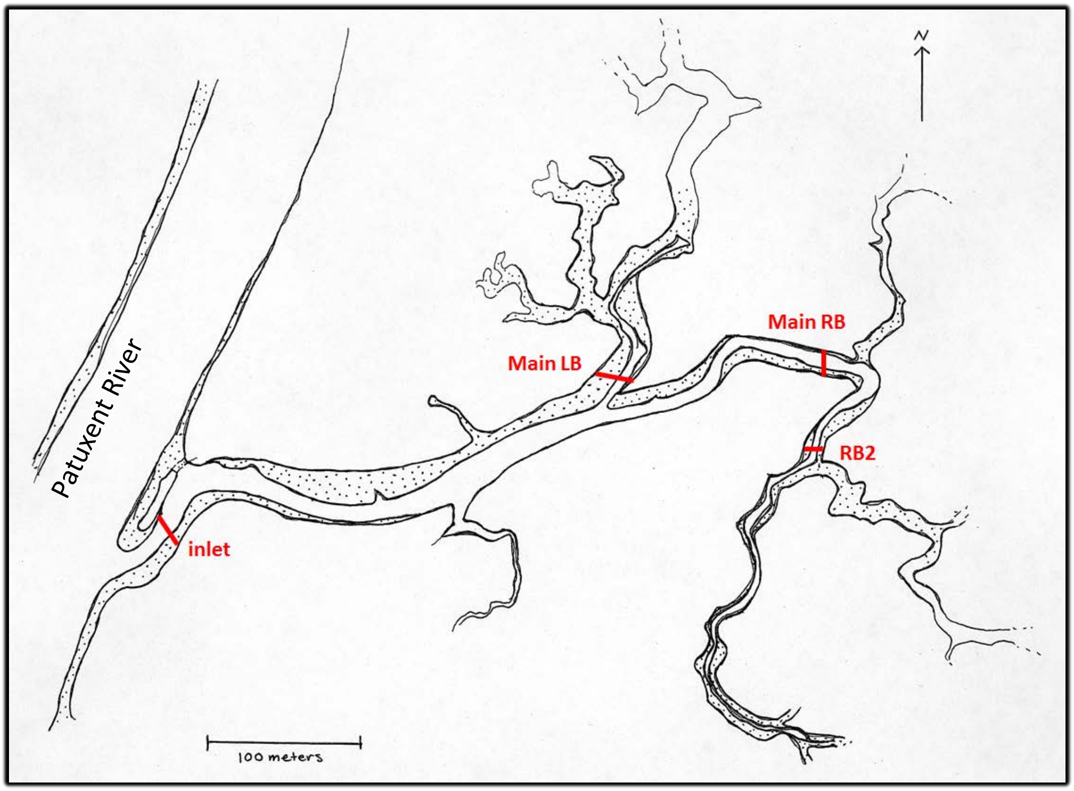

Figure 7: Map showing cross sectional locations used for potential sediment transport calculations

Hydrodynamic measurements at cross section locations were obtained from Statkiewicz (2014) and Prestegaard and Statkiewicz (unpublished data). Measurements of velocity, tidal stage, water surface gradient, and shear velocity were used in the Rouse equation to evaluate the vertical distribution of sediment of various grain sizes that could be carried in the channel.

Vertical distributions of suspended sediment by grain size

Sediment suspension occurs when the vertical turbulence, which is related to the shear velocity, is greater than the particle's fall velocity. Using a water surface gradient measurement collected by Statkiewicz 2014 and cross sectional depths measured in the field I calculated the shear velocity using equation (1). For any given cross section this was completed for both the maximum channel depth measured and for an average depth of the *Nuphar* bench. The *Nuphar* bench is the part of the cross section that is fairly flat for some distance due to the growth of *Nuphar* which likely prevents erosion, traps mineral sediment and contributes to the production of organic sediment. The fall velocity for any given grain size is then calculated using equation (2). With values obtained from equations (1) and (2) were used with equation (3) to determine the sediment concentration for various grain sizes at various depths using equation (4). Results of concentration from equation (4) were plotted against relative depth in the water column.

These vertical distributions of suspended sediment were calculated for the three main cross sections I measured this year and one cross section near the inlet measured by Statkiewicz in 2014.

Sediment sampling

Sediment core samples were collected in the *Nuphar* zone of the channel at sites adjacent to but not in the line of the cross sections. Sediment cores were retrieved by using a peat core sampler 50 cm in length and 5 cm in diameter. All sediment cores were retrieved from the *Nuphar* zone during low tide. Sampling locations were chosen at regular distances into the channel, into each main branch of the channel, and were constrained by accessibility. The core sampler was inserted until level with the surface of the sediment so that precisely the top 50 centimeters of sediment were retrieved. Cores were moved from the core sampler to polyvinylchloride pipe sleeves. These were made by sawing a 5 cm diameter pipe into 50 cm sections and then in half along their length. Once the cores were in the sleeves, they were wrapped in plastic wrap and then sealed in a plastic bag so that the form would be preserved. All the cores were kept in the freezer until they were to be analyzed so that no further decomposition occured after sampling.

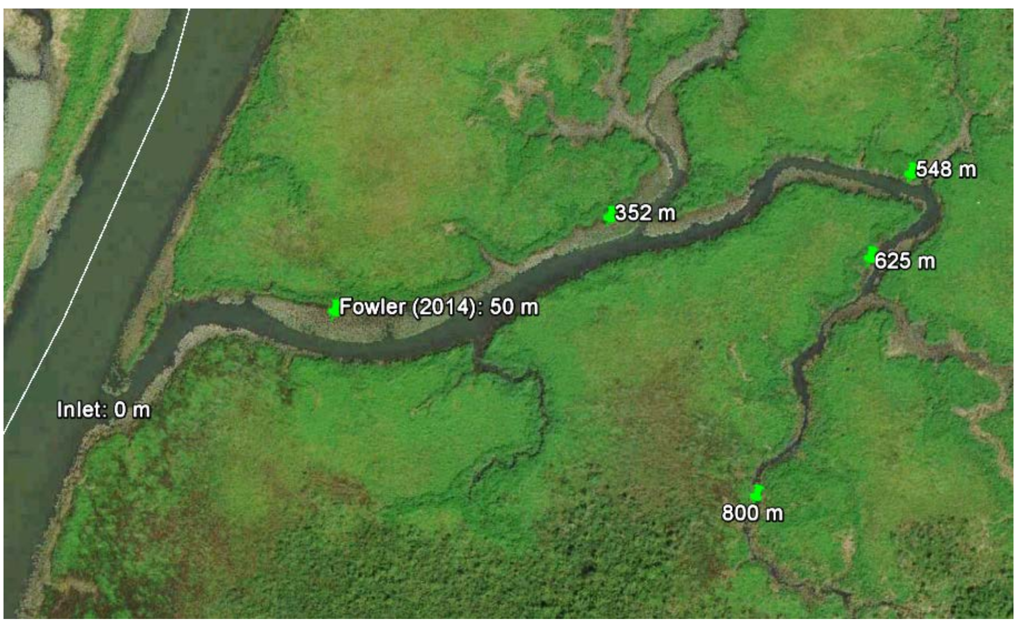

Figure 8: Locations at which analyzed sediment cores were retrieved within the marsh of study

Physical and Chemical Analyses of Sediment Cores

Core preparation and bulk density determination

The cores were removed from the freezer unwrapped and moved from the sleeve onto a sheet of plastic. The core was cut into 2.5 cm intervals using a thin blade, placed into ceramic dishes, and weighed on a mass balance. The samples were left on a table in the lab to air dry for 48 hours, and then placed in an oven set to 60^{0}C for 22 hours. This process removed all water from the sediment, and samples were weighed again. These dry weights were what were used to calculate bulk density:

$$\rho = \frac{mass}{volume}\left(\frac{g}{cm^3}\right)$$

Once dry, the samples were picked to remove large woody tissues then homogenized using a mortar and pestle. Between each sample the mortar and pestle were cleaned by grinding with baked sand, and then rinsed with ethanol, and dried with a heat gun. Homogenized samples were stored in labelled glass vials.

Combustion of organic matter

To calculate the proportion organic matter in the sample cores, the sediment is combusted. The homogenized sediment samples are weighed into 1g aliquots and placed in a kiln heated to 450ºC for 10 hours. This will cause all the organic matter to ignite and combust, creating carbon dioxide. After combustion the samples are weighed again to determine the mass lost to organic matter.

Carbon and nitrogen elemental and isotopic analyses

In order to perform nitrogen and carbon analyses on the core each sample had to be separated into two aliquots. A sample of mass 100 μg was necessary for the carbon analysis, and one of mass 2000 μg for the nitrogen analysis. This was done on a micro balance in a controlled environment as to ensure accuracy and precision, and aliquots were placed into tin capsules. 100 μg standards of urea, a material of known elemental composition, were also weighed and placed in line with the samples. These are to be used as a reference composition during analysis and as a determinant of the magnitude of error which is calculated as the standard deviation of the standards. A 10% precision range was necessary when weighing the samples; so, sample weights for urea were 100±10 μg, weights for carbon analysis were 100±10 μg, and weights for nitrogen analysis were 2000±200 μg.

The isotope analysis was performed in a stable isotopes laboratory using a *Euro EA Elemental Analyzer* and an *Isoprime isotope ratio mass spectrometer* with the guidance of lab manager Rebecca E. Plummer. Each sample, contained in its tin capsule, is loaded into the *Euro EA Elemental Analyzer* for the peripheral portion of the analysis. A tin capsule and its contents are dropped into a combustion/ oxidation column heated to 1040ºC. This column contains chromium oxide (CrO or Cr_2O_3) and silvered cobaltous/-ic oxide (Co_3O_4/ Ag), which serves to facilitate combustion and to consume impurities and halogens. Combustion of the sample produces carbon dioxide (CO_2), sulfate (SO_4), nitrogen in the form of nitrogen gas (N_2), nitrogen oxide (NO), or nitrogen dioxide (NO_2), and water vapor (H_2O). These gasses are then siphoned through a reduction column which contains reduced copper. This process removes any excess oxygen to form copper oxide; converting any nitrogen oxide (NO) or nitrogen dioxide (NO_2) to nitrogen gas (N_2). All gasses then travel through a column containing magnesium perchlorate ($Mg(ClO_4)_2$) which is a drying agent that removes all water vapor (H_2O). A gas chromatograph then separates the nitrogen gas (N_2) or the carbon dioxide (CO_2) from the remaining gasses based on their variant travel times through the equipment. Each gas is then transported to the *Isoprime isotope ratio mass spectrometer.* Here an ion source introduces electrons to the gas molecules giving them a charge. The molecules are then passed by an electromagnet. The isotopes of different masses are affected differently by the magnetic field, and the isotopes are separated. Each isotope is steered toward a separate collector containing a *Faraday cup*, which catches the charged particles in a vacuum where currents can be measured, indicating the amount of any isotope present in the sample. All samples were measured against lab standard tanks of CO_2 and N_2; nitrogen was standardized according to *VPDB*, and carbon was standardized according to *V-air*.

Results

Geomorphic Measurements

Channel width measurements determined from air photos are plotted in figure 6. This diagram indicates systematic variations in total channel width and open water width, the difference between the two is vegetated width. The channel width decreases systematically with distance upstream into the marsh. The portion of the channel covered with aquatic vegetation is at a maximum between the inlet and 300 meters upstream. *Nuphar*, the dominant aquatic plant in the channel, dies back in late fall.

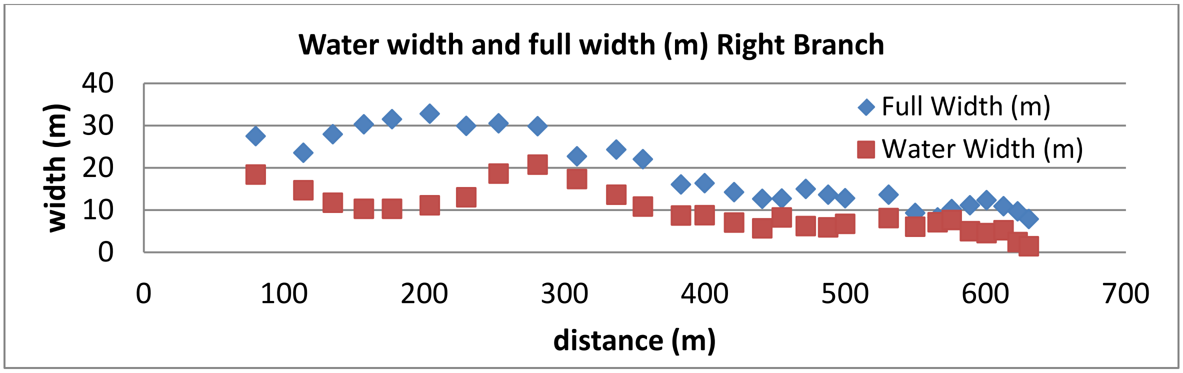

Figure 9: Total channel width and non-vegetated channel width as a function of the distance upstream (main channel and right branch channel).

Cross Sections

Cross sections were measured to determine the distribution of depths within the channel at locations near the acquired cores. The channel depths and previously obtained hydrodynamic data (Statkiewicz, 2014) were used in calculations of suspended sediment transport at various cross sections. While measuring the cross sections, the location of vegetation within the cross section was noted, so that the flow resistance from *Nuphar* can be taken into consideration for calculations. Four cross sections were used for sediment transport modeling. (Fig. 7)

Vertical distribution of suspended sediment and upstream travel distances

The calculations of the vertical distribution of suspended sediment made using the Rouse equation indicate that sand-sized sediment is only transported near the bed and thus is not transported onto the *Nuphar* platform. The Rouse calculations do not show substantial variation in sediment transport potential in various parts of the tidal channel. The main constraint on sediment type deposition will be the availability of that sediment to various elevations within the channel or marsh. For sediment to be deposited on the *Nuphar* bench that grain size will need to be able to be lifted high enough in the water column to reach the bench height. The Rouse calculations show that the fine sand sized particles are unlikely to be lifted high enough above the bed in the water column to be transported to heights above or equal to the *Nuphar* bench height and thus would not likely be transported on to the bench. The silt sized particles however can be transported onto the bench and will most likely be trapped by the vegetation. The two finest grain sizes appear to move as wash load and will likely be transported to all parts of the marsh. Any grain sizes larger than 420 microns are unlikely to be transported at all in this channel. The *Nuphar* depth calculations do not take into consideration flow resistance by vegetation and therefore are more representative of potential transport during the winter season of vegetation die back.

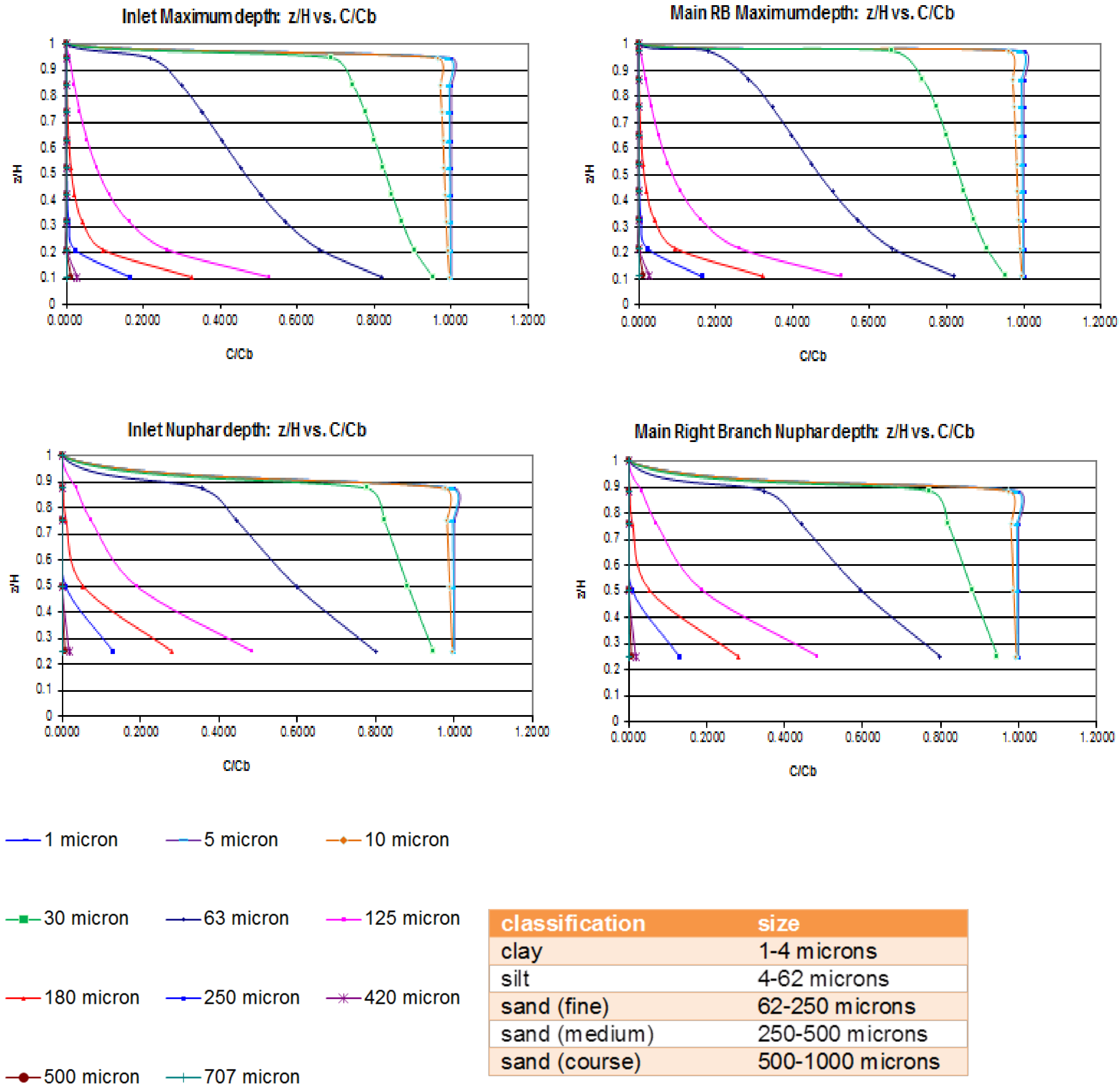

classification	size
clay	1-4 microns
silt	4-62 microns
sand (fine)	62-250 microns
sand (medium)	250-500 microns
sand (course)	500-1000 microns

Figure 10: Vertical distributions of suspended sediment concentration by grain size. Vertical relative concentrations were calculated with the Rouse equation for the cross section locations shown in figure 7.

The Rouse calculations of the verticial distribution of sediment of various grains sizes were combined with vertical distribution of velocity measurements recorded during a Spring (high) tide during vegetated conditions by Statkiewicz (2014). For each depth the sediment flux was calculated as the product of concentration and velocity (Figure 11). The depth at which the maximum flux was achieved for each grain size was used to identify the depth and thus flow velocity to use for transport distance calculations. Using these velocities, the maximum potential distance traveled during a tidal cycle was calculated (average distances could be significantly shorter). The calculations of transport distances show that the larger grain sizes are not able to travel as far as the smaller grain sizes (Figure 12), this is reflected in the sediment type found in the core samples.

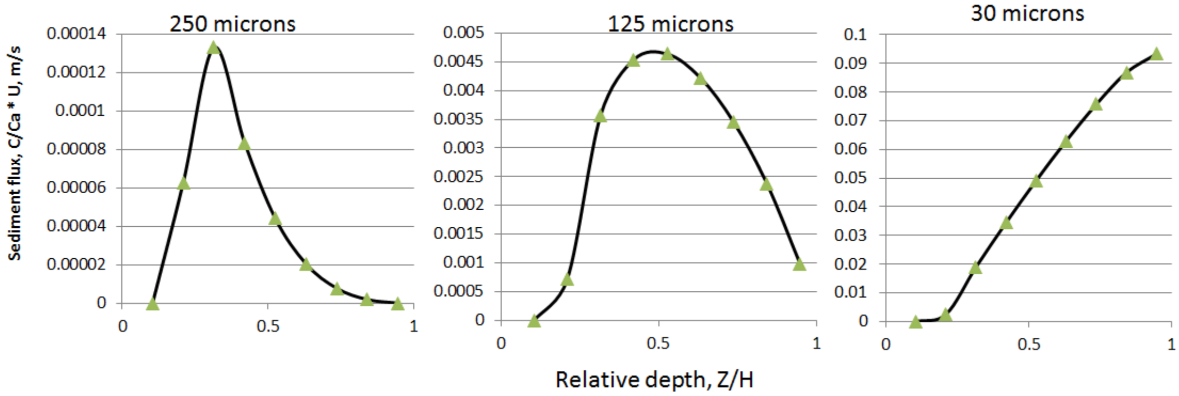

Figure 11: Peak flux calculations for sand and silt-sized particles.

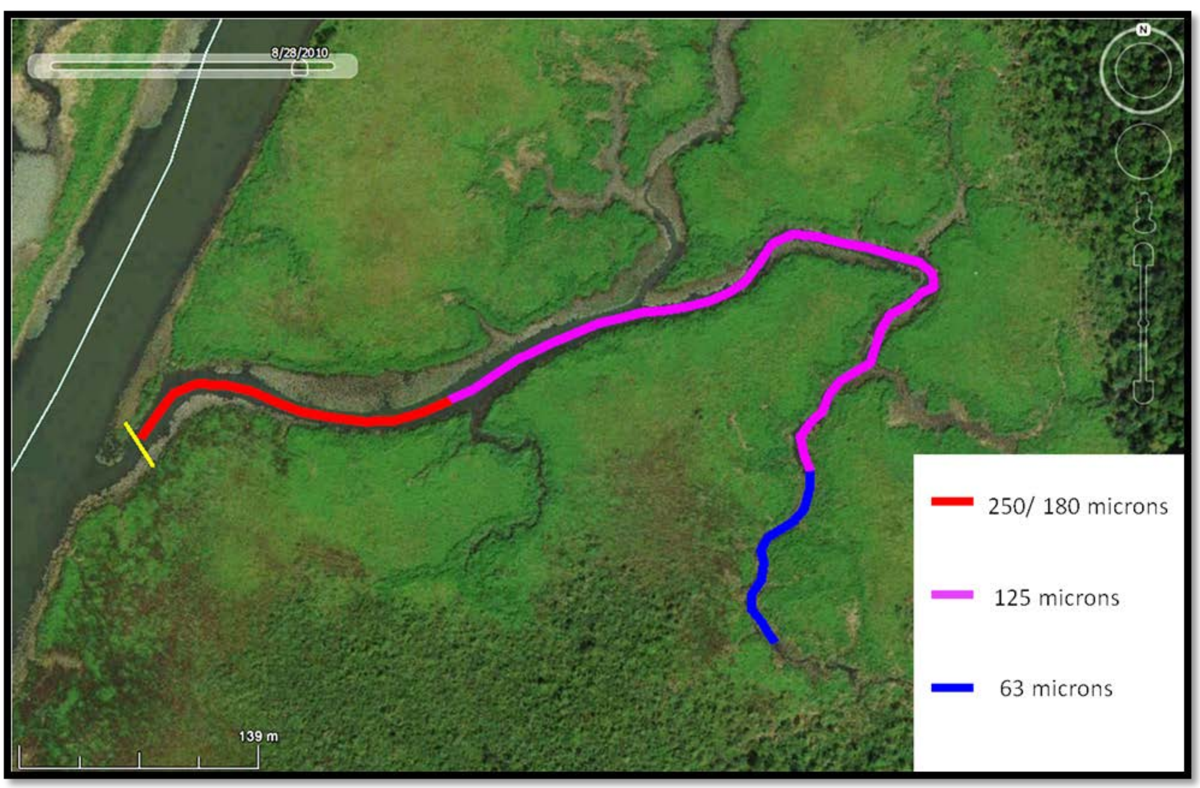

Figure 12: map of maximum potential transport distances during a Spring (high) tidal cycle for the indicated grain sizes. Grain size maximum distances: 250 & 180 microns = 202 meters; 125 microns= 680 meters; 63 microns= 800 meters.

Longitudinal Distribution of Sediment Bulk Density and Organic Carbon

Bulk density was calculated for four of the cores collected and percent organic matter was calculated for three of the cores collected. Data from the previous study by Fowler 2014 were included as well. The cores were chosen for their spatial relations within the channel network. The cores are spaced roughly consistently and span a significant portion of the main channel through the marsh. The core sediment becomes much more organic rich with increased distance from the inlet. This is consistent with the hypothesis that the upper reaches of the marsh channel network (greater distances from the inlet) will be composed of greater proportion organic matter, while closer to the inlet from the Patuxent sediment will be more mineral rich. This is also consistent with the predicted sediment transport potential in different parts of the marsh which show that even at the greatest possible flows only silt and clay sized sediment can be transported to the upper reaches of the marsh.

The bulk density has an inverse relationship to the percent organic matter which is to an extent to be expected because organic matter is less dense and more porous than lithic material. There is a clear trend of decreasing bulk density of the sediment with increased distance from the inlet. The surface bulk density could provide insight to how much organic material as opposed to lithic material has been deposited recently, presumably under the conditions currently observed at that location in the channel. The surface bulk densities roughly follow a similar trend to the average bulk density but there is some more variation. This is likely indicative of the channel form in relation to the sampling site. For example if the sample is taken on the outside of a bend where velocities would be slightly higher than the inside of a bend, there would be a slightly higher bulk density.

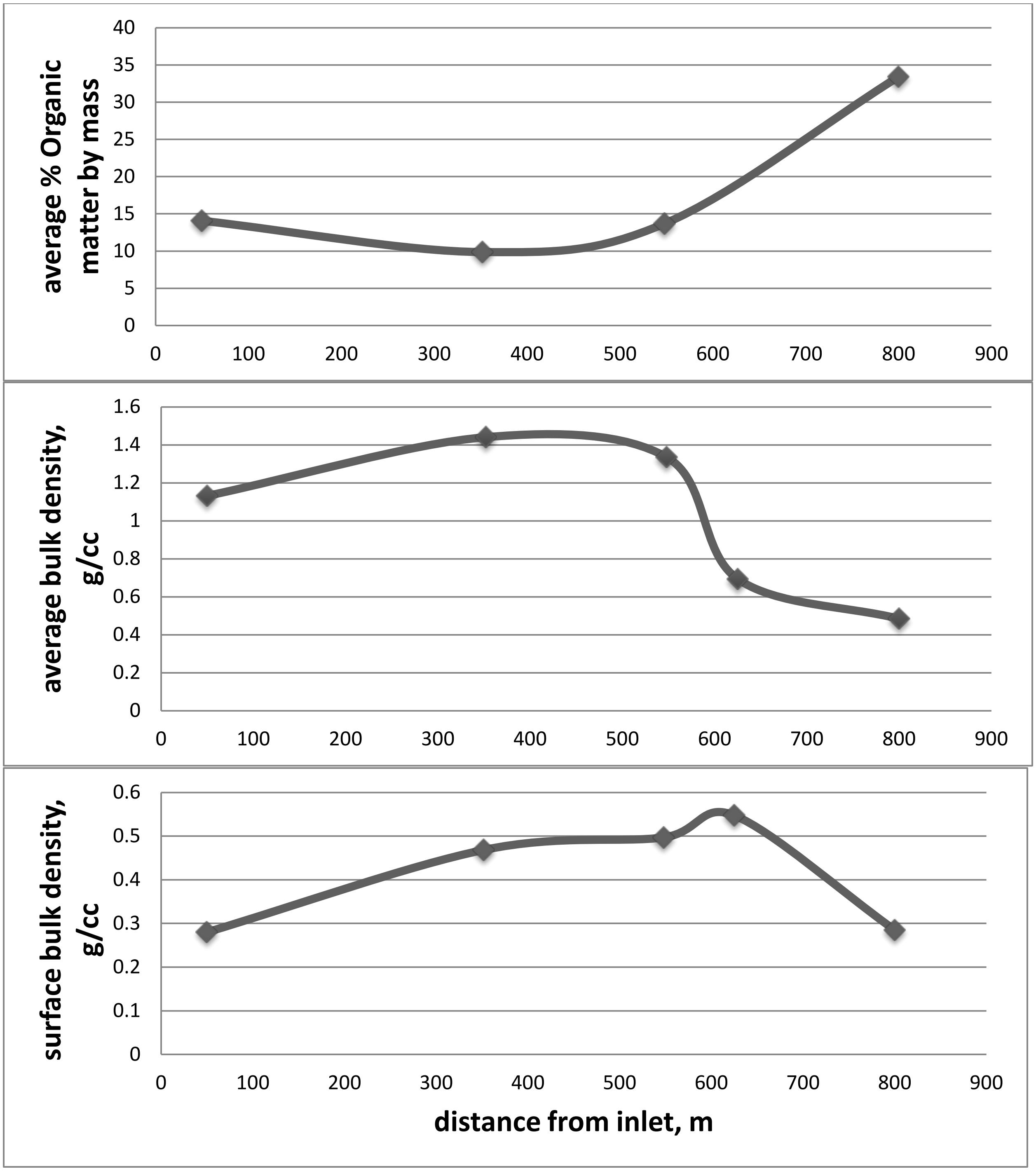

Figure 13: average percent organic matter by mass and average bulk density as a function of distance each core was retrieved from the inlet to the tidal channel network.

Temporal Variations in Sedimentation from Core Data

Inlet Core (Fowler, 2014)

The sediment core retrieved 50 meters from the tidal channel inlet, and analyzed by Fowler (2014) shows some interesting trends. The core has a bulk density between ~1.0 and ~1.5 g/cm^3 from a depth of 50cm to 20cm. From a depth of 15cm to the surface, the bulk density gradually decreases to a minimum surface bulk density of 0.28 g/cm^3. The total organic carbon gradually increases from a depth of 40cm to the surface ranging from 4.3 wt% to 22.8 wt%. The total nitrogen from a depth of 40cm to 20cm ranges around 0.3-0.6 wt%, but from a depth of 10 cm to the surface increases from ~1-1.4 wt%. The δ^{13}C values, from a depth of 40cm to 20cm, averages -27.65‰ then from a depth of 10cm to the surface decreases from -28.22‰ to -29.84‰. The d15N values from a depth of 35cm to 20 cm linger between 4.2-4.5‰, then there is a significant increase from 15cm depth at 6.12‰ to the surface at 7.78‰. (Fig. 14)

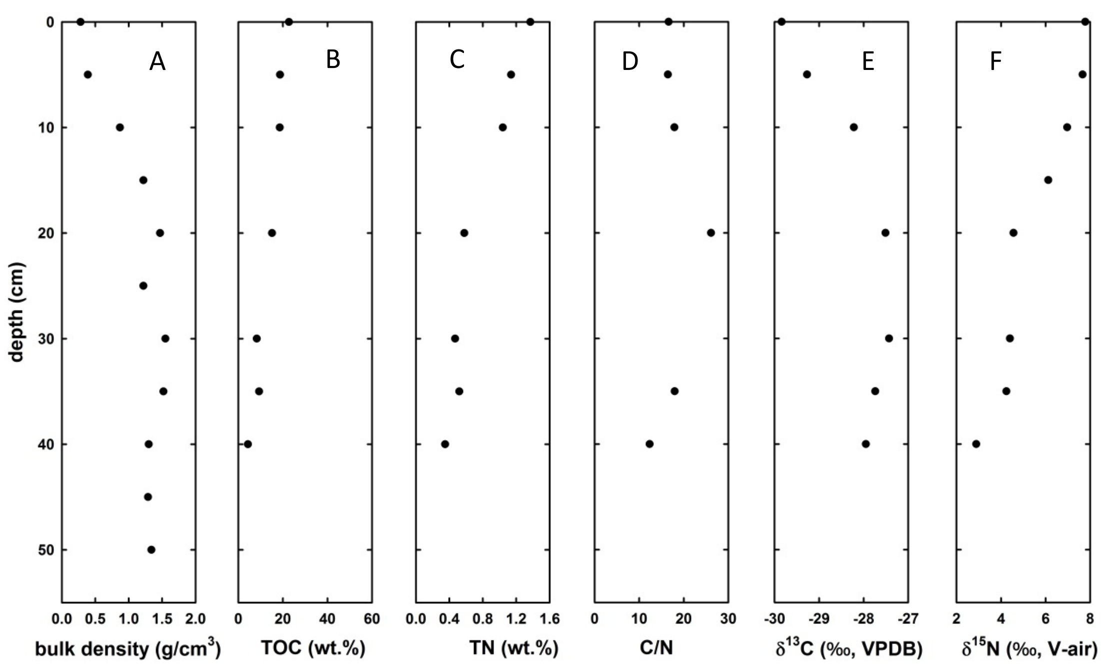

Figure 14: Core closest to the inlet, isotope analysis from (Fowler, 2014). A: core sediment bulk density (g/cc). B: Total organic carbon (weight %). C: Total nitrogen (weight %). D: Carbon to nitrogen ratio (C/N). E: ^{13}C elemental composition (ppm, VPDB). F: ^{15}N elemental composition (ppm, V-air).

Core retrieved 352 meters from the inlet

This core, retrieved 352 meters from the tidal inlet, has greatest bulk density between 40 and 15 cm depth. From 10 cm to the surface the bulk density gradually decreases. The total organic carbon ranges between 3.5 and 5.5 wt % for a majority of the core but increases to a maximum at the surface of 7.5 wt%. The total nitrogen ranges between 0.45 and 0.28 wt% until the top 5 cm of the core which averages 0.64 wt%. The $\delta^{13}C$ values vary quite sporadically but could be interpreted as gradually decreasing to the surface; values range between -27.3‰ and -28.8‰. The δ15N values from a depth of 50cm to 10cm range between 3.3‰ and 5.6‰ and in the top 15cm of the core is slightly greater increasing to the maximum of 5.9‰. (Fig. 15)

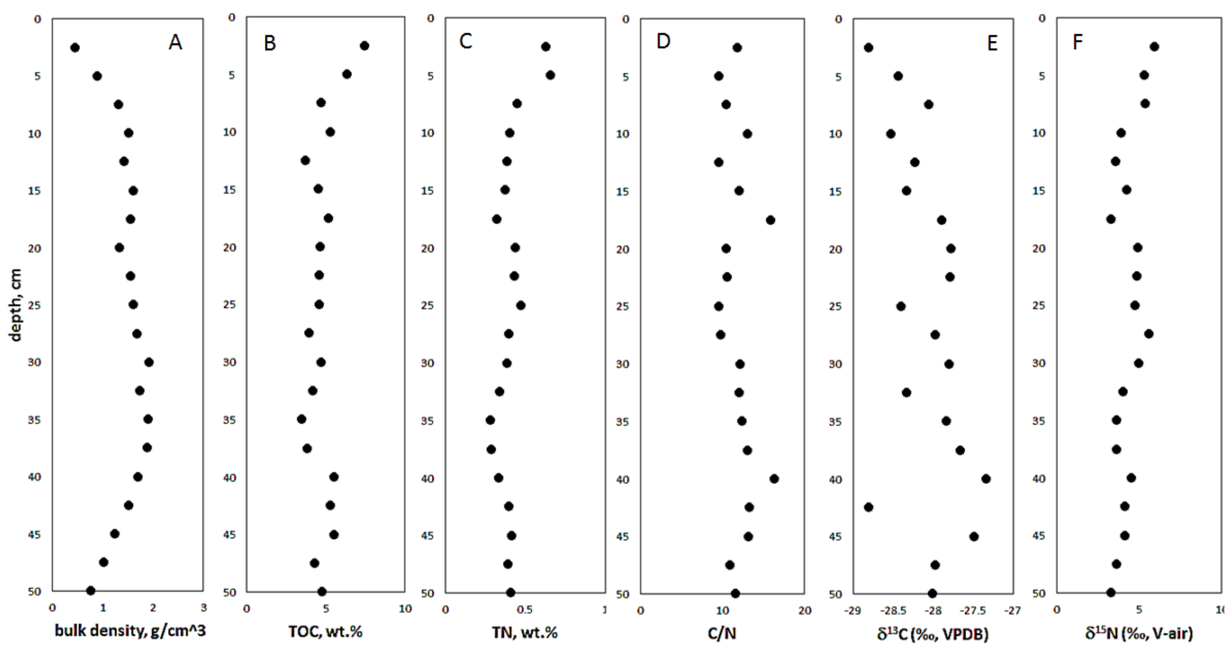

Figure 15: Intermediate distance from the inlet retrieved 352 meters from the inlet. Error: N=±0.13ppm, C=±0.06ppm. A: core sediment bulk density (g/cc). B: Total organic carbon (weight %). C: Total nitrogen (weight %). D: Carbon to nitrogen ratio (C/N). E: ^{13}C elemental composition (ppm, VPDB). F: ^{15}N elemental composition (ppm, V-air).

Core retrieved 800 m from the inlet

This core, retrieved furthest from the tidal channel inlet at a distance of 800 meters, shows some interesting values when compared with the inlet. Bulk density in this core is greatest at the greatest depths, from 40cm depth and greater. Above 40cm depth the bulk density is relatively consistent averaging 0.42 g/cm^3. The total organic carbon is also relatively homogenous from a depth of 32.5cm to the surface averaging 15 wt%, but from a depth of 40cm and down gradually decreases with a minimum of 6.5 wt%. the total nitrogen is consistent from a depth of 35cm to the surface averaging 1.26 wt%, then gradually decreases from a depth of 35 cm with 1.35 wt% downward to a minimum at 47.5cm depth of 0.53 wt%. δ^{13}C values are on average -28‰ from a depth of 50cm to a depth of 35 cm, and on average -29‰, from above 35cm depth to the surface. The δ^{15}N values average 3.7‰ between depths of 50-45cm, then gradually increase from 3‰ at 42.5cm depth to 7.3‰ at 27.5cm depth, then from 25cm depth to the surface average 5.58‰. The δ^{34}C values seem to generally increase with depth. (Fig. 16)

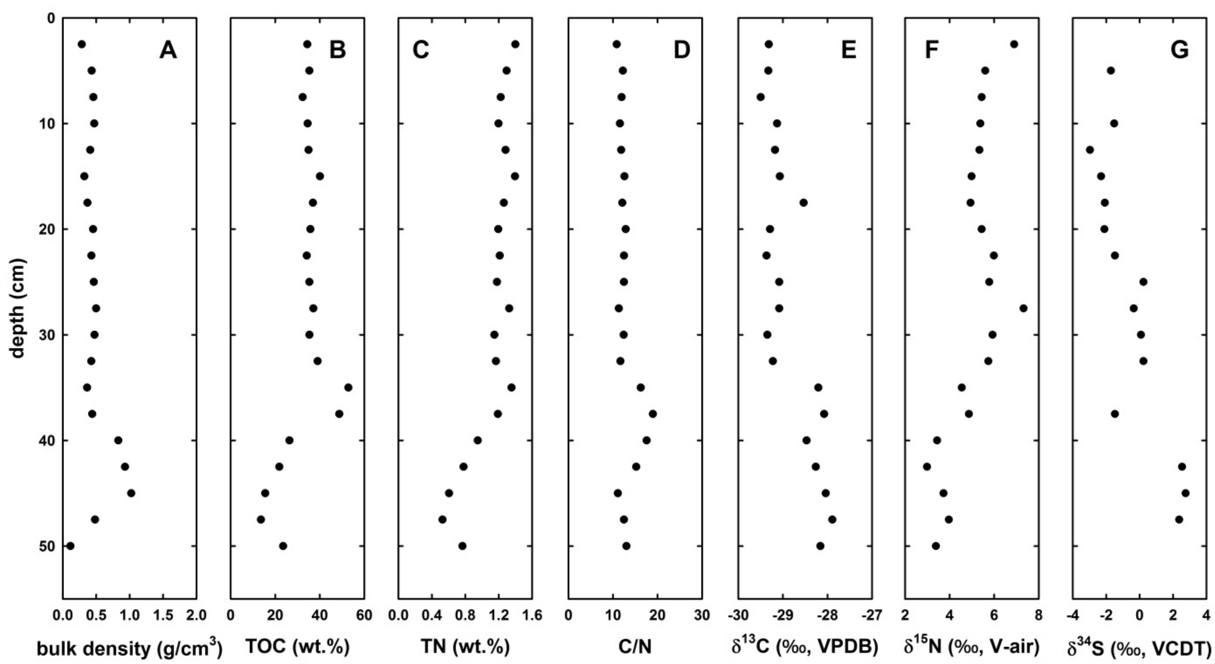

Figure16: Core furthest from the inlet. Error N= ±0.13 ppm, C= ±0.04ppm. A: core sediment bulk density (g/cc). B: Total organic carbon (weight %). C: Total nitrogen (weight %). D: Carbon to nitrogen ratio (C/N). E: ^{13}C elemental composition (ppm, VPDB). F: ^{15}N elemental composition (ppm, V-air). G: ^{34}S analyses performed by Dr. Alan Jay Kaufman.

Discussion and Implications

As can be seen based on the calculation of average bulk density and average percent organic matter, some clear trends have emerged that support my initial hypothesis on spatial variation of sediment type within the marsh (hypothesis 1). With increased distance into the marsh we observe a significant decrease in bulk density along with a significant increase in percent organic matter. This is likely a result of the phenomena modeled by the transport calculations which indicate a very limited potential transport distance for mineral sediment. The cores also show a decrease in bulk density and increase in organic sediment near the surface. This could be a reflection of an increase in vegetation within the marsh which would increase organic matter production and decrease the ability to transport mineral sediment out of the channel onto the *Nuphar* bench, or it could be a seasonally eroded organic layer.

The cores retrieved 50 and 352 meters from the inlet have significantly higher bulk density than the core retrieved 800 meters from the inlet. All cores display a decrease in bulk density and increase in organic carbon near the surface but these shifts occur at very different depths. The top 25 cm of the upper marsh core appears relatively homogeneous. This could be due to the low bulk density and high organic matter content of the upper portion of this core. The light organic matter behaves differently than lithic matter as described by Larsen et al; "Highly organic floc is more mobile than less organic floc, which has implications for ecosystem metabolism, materials cycling, and even landscape evolution." (Larsen, Harvey, & Crimaldi, 2009) The transport of light organic material was actively observed during time spent in the marsh collecting samples.

Increases in bulk density and decreases in organic carbon with depth in each core could indicate a significant shift from mineral sediment accumulation to organic sediment accumulation. Within the last 50-100 years there has been a large increase in agricultural and urban land use within the basin. With increased urbanization, infiltration rates are lower so there is greater runoff during storm events and more sediment carried to the waterways. Due to higher velocities and increased opacity of the water (large sediment loads and epiphyton shading), there was a great decrease in the amount of submerged vegetation because these conditions were not conducive to their growth. This time would be reflected in the section of the cores where mineral sediment is high and organic matter is low. Over time agricultural practices were improved to reduce overland sediment washing with runoff and the Brighton Damn of the Patuxent River, built in 1943, has also decreased sediment fluxes into the water system. There is a significant decrease in mineral sediment beginning at about 20 cm depth in both the inlet and the intermediate core. If this is assumed to be 1943, the average accumulation rate would be 2.7 mm a year, which would parallel the average sea level rise rate.

Nitrogen rich fertilizers which have an isotopic composition equal to atmospheric nitrogen composition can runoff of farm lands directly to the waterways or can infiltrate and travel as through flow or with the water table until it contributes to the base flow of the waterway. This longer path, which would be more likely since improved farming practices, allows for denitrification by vegetation and bacteria. This would enrich the base flow in heavier isotopes of nitrogen as is reflected in the apparent increase of heavy nitrogen isotopes over time. This increase in $\delta^{15}N$ is apparent in all the cores analyzed. If the $\delta^{15}N$ levels were reflecting decomposition of organic matter over time we should see the opposite trend where with increased depth $\delta^{15}N$ levels also increase. This is strong evidence of environmental changes within the system throughout the past.

Results from analysis of the core retrieved furthest from the inlet shows a decrease in $\delta^{15}N$ at a greater depth than observed by Fowler (2014). This core is also much higher in organic sediment. The $\delta^{15}N$ composition in the upper portion of the core is however lower than the $\delta^{15}N$ composition of the core analyzed by Fowler (2014). This could result from differences in initial $\delta^{15}N$ composition that could reflect transport of water, sediment, and nutrients into the marsh as suggested by Jenner (2010). This might suggest that less new nitrogen rich water reaches this greater distance into the channel. Another possible cause for these shifts would be the type of sediment present. Mineral sediment, more prevalent in this core, would not be as easily transported. The upper marsh core that shows consistent isotopic composition for a majority of the upper part of the core could be only a seasonal deposition. The organic matter at the top of the core may be eroded away and re-deposited each year, and the net annual accumulation could in fact be consistent with the inlet measurements and sea level rise (Figure 17).

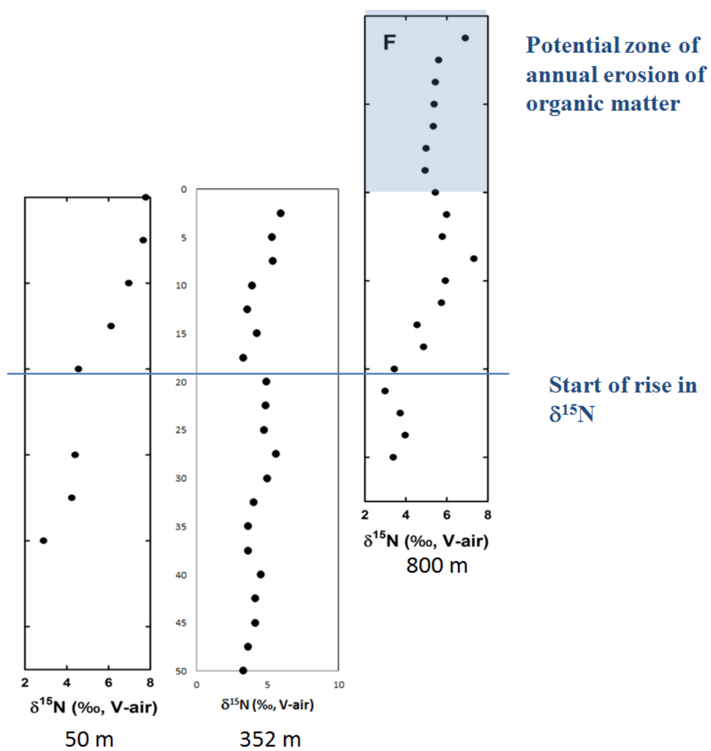

Figure 17: temporal comparison of shifts in d15N from the different sampling sites suggests a possible seasonally eroded layer.

This data has provided a platform for understanding the behavior of this freshwater tidal marsh but poses some interesting questions. I would suggest further investigation into the temporal relationships of geochemical observations observed within sediment cores taken from this marsh. However, based on these observations and the observations of others it would appear as though this tidal marsh channel is adequately adapting to the current sea level rise rate.

References

Boynton, W. R., Hagy, J. D., Cornwell, J. C., Kemp, W. M., Greene, S. M., Owens, M. S., et al. (2008). Nutrient Budgets and Management Actions in the Patuxent River Estuary, Maryland. *Estuaries and Coasts*, 623-651.

D'Alpaos, A., Lanzoni, S., Mudd, S. M., & Fagherazzi, S. (2006). Modeling the influence of hydroperiod and vegetation on the cross-sectional formation of tidal channels. *Estuarine, Coastal and Shelf Science*.

Fagherazzi, S., & Sun, T. (2004). A stochastic model for the formation of channel networks in tidal marshes. *Geophysical Research Letters*.

Fisher, T. R., HagyIII, J. D., Boynton, W., & Williams, M. R. (2006). Cultural eutrophication in the Choptank and Patuxent estuaries of Chesapeak Bay. *Limnology and Oceanography,* 435-447.

Fowler, E. (2014). *Carbon and Nitrogen Abundance, Isotope Fractionation, and Aquatic vegitation decay rates in Patuxent Freshwater Wetlands.*

Friedrichs, C. T., & Perry, J. E. (2001). Tidal Marsh Morphodynamics: A Synthesis. *Coastal Education & Research Foundation, Inc.*, 7-37.

Gribsholt, B., & Boschker, H. T. (2005). Nitrogen procssing in a tidal freshwater marsh: A whole-ecosystem 15N labeling study. *Limnol.Oceanogr.*

Jenner, B. A. (2010). *Geomorphic and hydrologic controls on tidal prism and inlet cross setional area for Chesapeake Bay lagoons.*

Jenner, B. A. (2011). *Geomorphic and hydrologic controls on tidal prism and inlet cross setional area for Chesapeake Bay lagoons.*

Kearney, M. S., & Stevenson, J. C. (1991). Island Land Loss and Marsh Vertical Accretion Rate Evidence for Historical Sea-Level Changes in Chesapeake Bay. *Journal of Coastal Research*, 403-415.

Larsen, L. G., Harvey, J. W., & Crimaldi, J. P. (2009). Morphologic and transport properties of natural organic floc. *Water Resources Research*, Vol. 45 .

Leonard, L. A., & Luther, M. E. (1995). Flow hydrodynamics in tidal marsh canopies. *American Society of Limnology and Oceanography*, *40*(8), 1474-1484.

Leonard, L. A., & Reed, D. J. (2002). Hydrodynamics and Sediment Transport Through Tidal Marsh. *Journal of Coastal Research*(36), 459-469.

Mitsch, W. J., & Gosselink, J. G. (2000, October). The value of wetlands: importance of scale and landscape setting. *Ecological Economics*, pp. 25-33.

Neph, H., & Ghisalberti, M. (2008). Flow and transport in channels with submerged vegetation. *Acta Geophysica*, pp. 753-777.

Rouse, H. (1937). Modern Conceptions of the Mechanics of Fluid Turbulence. *Transactions of the American Society of Civil Engineers*, 463-505.

Seldomridge, E., & Prestegaard, K. (2012). Use of geomorphic, hydrologic, and nitrogen mass balance data to model ecosystem nitrate retention in tidal freshwater wetlands. *Biogeosciences*.

Seldomridge, E., & Prestegaard, K. (2014). Geochemical, Temperature, and Hydrologic Transport Limitations on Nitrate Retention in Tidal Freshwater Wetlands, Patuxent River, Maryland. *Wetlands*, 641-651.

Statkiewicz, A. E. (2014). *Vegitation-hydrodynamic interactionsand the stability of channel inlets in tidal freshwater wetlands, Chesapeake Bay system* .

Tambroni, N., & Seminara, G. (2012). A one-dimensional eco-geomorphic model of mmarsh response to sea level rise: Wind effects, dynamics of the marsh border and equilibrium. *Journal of Geophysical Research*.

Temmerman, S., Bouma, T., Koppel, J. V., Wal, D. V., Vries, M. B., & J.Herman, P. M. (2007). Vegetation causes channel erosion in a tidal landscape. *Geology*, pp. 631-634.

Temmerman, S., Bouma, T., Koppel, J. V., Wal, D. V., Vries, M. D., & Herman, P. M. (2007). Vegetation causes channel erosion in a tidal landscape. *Geology*, 631-634.

Walter, B., Gromke, C., & Lehning, M. (2012). Shear-Stress Partitioning in Live Plant Canopies and Modifications to Raupach's Model. *Boundary-Layer Meteorol*, 217-241.

Appendix

Cross Sections:

RB3		
distance (ft)	width (m)	depth (m)
2.5	0.762	0R
3	0.9144	0.05
4	1.2192	0.03
5	1.524	0.08
6	1.8288	0.54
7	2.1336	0.52
8	2.4384	0.54
9	2.7432	0.55
10	3.048	0.48
11	3.3528	0.4
12	3.6576	0.43
13	3.9624	0.47
14	4.2672	0.33
15	4.572	0.28
16	4.8768	0.2
17	5.1816	0.12
18	5.4864	0.13
19	5.7912	0.12
20	6.096	0.15
21	6.4008	0.16
22	6.7056	0.22
23	7.0104	0.38
24	7.3152	0.54
25	7.62	0.7
26	7.9248	0.79
27	8.2296	0.86
28	8.5344	0.89
29	8.8392	0.8
30	9.144	0.65
31	9.4488	0.54
32	9.7536	0.52
33	10.0584	0.46
34	10.3632	0.36
35	10.668	0.31
36	10.9728	0.27
37	11.2776	0.26
38	11.5824	0.22
39	11.8872	0.2
40	12.192	0.2
41	12.4968	0.16
42	12.8016	0.1
43	13.1064	0.05

main channel A	538m	
width (ft)	width (m)	depth (m)
2.5	0.762	0.25
3	0.9144	0.275
6	1.8288	0.5
9	2.7432	0.48
12	3.6576	0.7
15	4.572	0.79
18	5.4864	0.85
21	6.4008	1.48
24	7.3152	1.6
27	8.2296	1.73
30	9.144	1.85
33	10.0584	1.8
36	10.9728	1.2
39	11.8872	1.38
42	12.8016	0.85
45	13.716	0.51
48	14.6304	0.5
51	15.5448	0.35
54	16.4592	0.32
56	17.0688	0.38

RB2	625m	
width (ft)	width (m)	depth (m)
2.5	0.762	0.02
3	0.9144	0.03
4	1.2192	0.16
5	1.524	0.2
6	1.8288	0.22
7	2.1336	0.38
8	2.4384	0.55
9	2.7432	0.65
10	3.048	0.68
11	3.3528	0.62
12	3.6576	0.7
13	3.9624	0.85
14	4.2672	1.09
15	4.572	1.32
16	4.8768	1.31
17	5.1816	1.35
18	5.4864	1.39
19	5.7912	1.44
20	6.096	1.43
21	6.4008	1.42
22	6.7056	1.41
23	7.0104	1.45
24	7.3152	1.44
25	7.62	1.36
26	7.9248	1.36
27	8.2296	1.27
28	8.5344	1.21
29	8.8392	1.13
30	9.144	0.98
31	9.4488	1
32	9.7536	0.45
33	10.0584	0.42
34	10.3632	0.18
35	10.668	0.12
36	10.9728	0.1
37	11.2776	0.1
38	11.5824	0.05
39	11.8872	0.06
40	12.192	0.05

RBT		
width (ft)	width (m)	depth (m)
2.5	0.762	L0
3	0.9144	0.06
4	1.2192	0.18
5	1.524	0.22
6	1.8288	0.23
7	2.1336	0.31
8	2.4384	0.4
9	2.7432	0.71
10	3.048	0.73
11	3.3528	0.72
12	3.6576	0.68
13	3.9624	0.7
14	4.2672	0.7
15	4.572	0.73
16	4.8768	0.82
17	5.1816	0.84
18	5.4864	0.81
19	5.7912	0.73
20	6.096	0.65
21	6.4008	0.65
22	6.7056	0.62
23	7.0104	0.63
24	7.3152	0.61
25	7.62	0.565
26	7.9248	0.565
27	8.2296	0.56
28	8.5344	0.56
29	8.8392	0.56
30	9.144	0.53
31	9.4488	0.525
32	9.7536	0.525
33	10.0584	0.5
34	10.3632	0.46
35	10.668	0.42
36	10.9728	0.41
37	11.2776	0.37
38	11.5824	0.33
39	11.8872	0.29
40	12.192	0.22
41.3	12.58824	0.12

RB1		
width (ft)	width (m)	depth (m)
2.5	0.762	0.18
3	0.9144	0.21
4	1.2192	0.22
5	1.524	0.25
6	1.8288	0.3
7	2.1336	0.4
8	2.4384	0.38
9	2.7432	0.42
10	3.048	0.43
11	3.3528	0.41
12	3.6576	0.39
13	3.9624	0.38
14	4.2672	0.39
15	4.572	0.36
16	4.8768	0.33
17	5.1816	0.3
18	5.4864	0.29
19	5.7912	0.32
20	6.096	0.39
21	6.4008	0.39
22	6.7056	0.4
23	7.0104	0.5
24	7.3152	0.5
25	7.62	0.55
26	7.9248	0.58
27	8.2296	0.5
28	8.5344	0.72
29	8.8392	0.76
30	9.144	0.83
31	9.4488	0.95
32	9.7536	1
33	10.0584	1
34	10.3632	1
35	10.668	0.93
36	10.9728	0.72
37	11.2776	0.56
38	11.5824	0.49
39	11.8872	0.45
40	12.192	0.31
41	12.4968	0.25
42	12.8016	0.16
43	13.1064	0.12

MainLB	388m	
width (ft)	width (m)	depth (m)
2.5	0.762	0.2
3	0.9144	0.27
6	1.8288	0.36
9	2.7432	0.56
12	3.6576	0.52
15	4.572	0.55
18	5.4864	0.58
21	6.4008	0.65
24	7.3152	0.57
27	8.2296	0.62
30	9.144	0.63
33	10.0584	0.62
36	10.9728	0.61
39	11.8872	0.6
42	12.8016	0.78
45	13.716	0.65
48	14.6304	0.63
51	15.5448	0.79
54	16.4592	0.95
57	17.3736	1.16
60	18.288	1.3
63	19.2024	1.34
66	20.1168	1.2
69	21.0312	1.05
72	21.9456	1.05
73	22.2504	0.95
75	22.86	0.56
78	23.7744	0.42
81	24.6888	0.35
84	25.6032	0.12
87	26.5176	0.15
89	27.1272	0.08

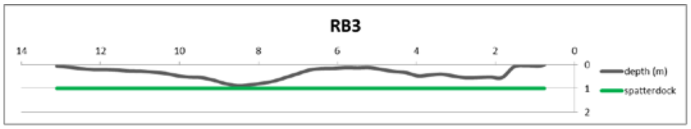

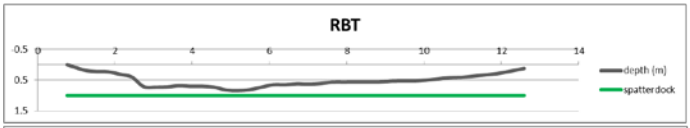

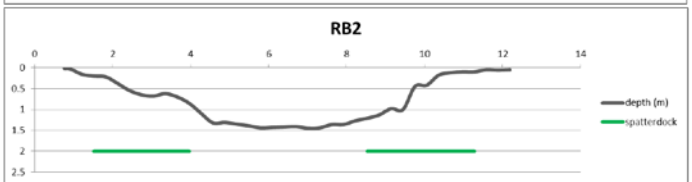

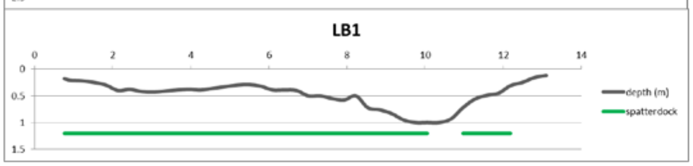

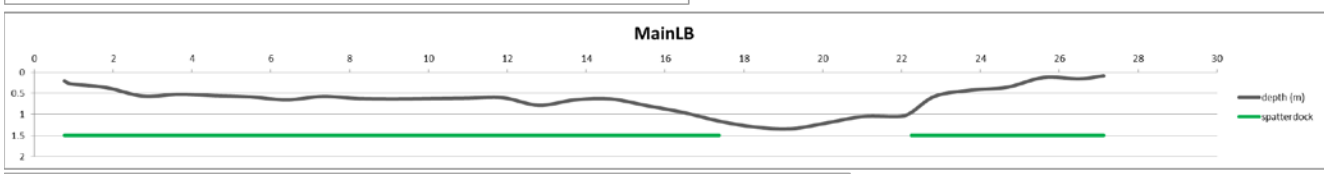

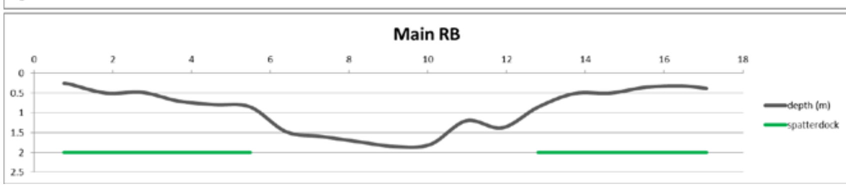

Morphology and Hydrodynamic Data from Statkiewicz (2014):

			Measurement station:			
	9.29.13		Station 36 ft (11 m)			
	Velocity Profile center of LM1 cross section, Nuphar Marsh					
			Maximum depth = 1.89 m			
			tidal cycle		ave	max
d, m	Z/D	v, m/s	Ave v	Duration, hr	distance	distance
0.3	0.16	0	0	hrs	m	m
0.47	0.25	0.0125	0.00695455	4.5	112.663636	202.5
0.76	0.40	0.026	0.0176	4	253.44	374.4
0.86	0.46	0.045	0.02227273	3.35	268.609091	542.7
0.95	0.50	0.054	0.02181818	3.5	274.909091	680.4
1.13	0.60	0.075	0.03545455	3	382.909091	810
1.32	0.70	0.095	0.03181818	2.5	286.363636	855
1.51	0.80	0.111	0.02909091	2	209.454545	799.2
1.85	0.98	0.14	0.01909091	0.74	50.8581818	372.96

								0.054864		incoming	incoming			INCOMING		0.002333333
	15:45	15:45	13:00	13:00			gh 2.40	13:00	15:45	13:00	13:00	13:00	15:45	13:00	13:00	13:00
veg	q	a	q	area, m2	sta	sta, m	depth, m	depth, m	DEPTH,M	Us ft/s	Us m/s	u/u*	u/u*	t, n/M2	Eff Zo	log d/zo
mv					1	0.3048	0.28							0	0	
mv	0	0.0762		0.082296	3	0.9144	0.29	0.27	0.25		0	0	0	0.3179736	3.703703704	0
sp	0	0.2286	0	0.246888	6	1.8288	0.29	0.27	0.25		0	0	2.606341647	0.3179736	3.703703704	0
sp	0.0045339	0.10668	0	0.112014	7	2.1336	0.49	0.465	0.45		0	0	1.295101577	0.5476212	2.150537634	0
sp	0.00919734	0.324612	0	0.333756	9	2.7432	0.655	0.63	0.615		0	0	1.490590047	0.7419384	1.587301587	0
sp	0.02553449	0.669798	0	0.683514	12	3.6576	0.89	0.865	0.85		0	0	1.80748593	1.0186932	1.156069364	0
	0.0615549	1.1326368	0	1.1478768	16	4.8768	1.048	1.018	1.008		0	0	1.918502005	1.19887824	0.982318271	0
	0.04112722	0.6547104	0	0.6608064	18	5.4864	1.18	1.15	1.14		0	0	2.528297251	1.354332	0.869565217	0
	0.09680314	1.099566	0	1.10871	21	6.4008	1.305	1.275	1.265		0	0	3.014397589	1.501542	0.784313725	0
	0.1390184	1.2573	0.02909398	1.266444	24	7.3152	1.525	1.495	1.485		0.027027027	0.644115915	2.40430978	1.7606316	0.865723021	0.112020159
	0.14372865	1.504188	0.04704889	1.513332	27	8.2296	1.845	1.815	1.805	0.12	0.036576	0.791123425	2.733118894	2.1374892	0.756327782	0.137586683
	0.19929312	1.664208	0.07264758	1.673352	30	9.144	1.875	1.845	1.835	0.167571429	0.051075771	1.095728858	2.21048377	2.1728196	0.840553131	0.19056154
	0.16050851	1.643634	0.08552189	1.650492	33	10.0584	1.8	1.765	1.76	0.2	0.06096	1.337084806	2.428043645	2.0786052	0.967813728	0.232536488
	0.17362607	1.652778	0.10415353	1.6580358	36	10.9728	1.895	1.8615	1.855	0.242463415	0.073902849	1.578396138	1.944132903	2.19225132	1.010742752	0.274503676
	0.14430424	1.671066	0.13945436	1.6763238	39	11.8872	1.84	1.805	1.8	0.3211	0.09787128	2.122770361	2.094132626	2.1257124	1.296284261	0.369177454
	0.14578522	1.591056	0.14283841	1.595628	42	12.8016	1.72	1.685	1.68	0.345525	0.10531602	2.364181616	1.804720403	1.9843908	1.529544494	0.41116202
	0.11440163	1.499616	0.19874956	1.504188	45	13.716	1.64	1.605	1.6	0.51	0.155448	3.575476851	1.48136927	1.8901764	2.608236837	0.621822061
	0.08577397	1.403604	0.18812892	1.40589	48	14.6304	1.51	1.47	1.47	0.5165	0.1574292	3.783667558	1.545484505	1.7311896	3.09536456	0.658029141
	0.07823033	1.28016	0.14364281	1.28016	51	15.5448	1.37	1.33	1.33	0.433097561	0.132008137	3.335502191	2.259984826	1.5663144	2.859141812	0.580087338
	0.09369628	1.1023092	0.09424347	1.1023092	54	16.4592	1.121	1.081	1.081	0.33	0.100584	2.819047578	1.474584197	1.27307208	2.860509867	0.490269144
sp	0.04631436	0.9262872	0.05347978	0.9240012	57	17.3736	0.985	0.94	0.945	0.2234	0.06809232	2.046541496	1.57712646	1.1070192	2.414306516	0.35592026
sp	0.0424053	0.848106	0.02437813	0.843534	60	18.288	0.95	0.905	0.91		0.034	1.041456123	1.050841703	1.0658004	1.676772817	0.181122804
sp	0.02570871	0.786384	0.00662597	0.779526	63	19.2024	0.85	0.8	0.81		0.01	0.325792706	1.316334165	0.942144	1.424195516	0.056659601
sp	0.02808663	0.726948	0.01708374	0.717804	66	20.1168	0.82	0.77	0.78		0.028	0.92982029	0.922218997	0.9068136	1.884591167	0.161707877
sp	0.01967389	0.740664	0.02673706	0.73152	69	21.0312	0.88	0.83	0.84		0.043	1.375358005	0.917339315	0.9774744	2.089847539	0.239192697
sp	0.02030853	0.740664	0.02479396	0.729234	72	21.9456	0.82	0.765	0.78		0.04	1.332648528	1.180440316	0.9009252	2.228966422	0.231764961
sp	0.02471623	0.726948	0.02121865	0.713232	75	22.86	0.85	0.795	0.81		0.035	1.143854619	1.447967581	0.9362556	1.988676352	0.198931238
sp	0.03050667	0.717804	0.01968555	0.701802	78	23.7744	0.8	0.74	0.76		0.033	1.117852314	2.299753006	0.8714832	2.114352426	0.194409098
p	0.04304714	0.658368	0	0.64008	81	24.6888	0.72	0.66	0.68		0	0	0	0.7772688	1.515151515	0
p	0	0.306324	0	0.310896	82.5	25.146	0.7	0.7	0.66		0	0	0	0.824376	1.428571429	0
p	0	0.27432	0	0.292608	84	25.6032	0.58	0.58	0.54		0	0	0	0.6830544	1.724137931	0
p	0	0.4572	0	0.493776	87	26.5176	0.5	0.5	0.46		0	0	0	0.58884	2	0
mv	0	0.370332	0	0.406908	90	27.432	0.39	0.39	0.35		0	0	0	0.4592952	2.564102564	0
mv	0	0.179832	0	0.204216	92	28.0416	0.28	0.28	0.24		0	0	0	0.3297504	3.571428571	0
mv	0	0.057912	0	0.070104	93	28.3464	0.18	0.18	0.14		0	0	0	0.2119824	5.555555556	0
mv	0	0.06858	0	0.086868	94.5	28.8036	0.2	0.2	0.16		0	0	0	0.235536	5	0
	1.99788486	29.0731956	1.43952624	29.2658292												

				OUT				outgoing	outgoing	outgoing	outgoing	
13:00	15:45	13:00	15:45	15:45			16:00	15:45	15:45	15:45	15:45	
d/zo	d/zo	Zo	Zo	T, n/M2	eff t N/m2	u"	T, N/m2	Us, ft	Us m/s	Um m/s	D gh	U m/s
1	1	0.27	0.25	0.368025	0	0	0.58884		0	0	0.02	0
1	2.839728421	0.27	0.088036588	0.368025	0	0	0.58884		0	0	0.02	0
1	1.679712897	0.465	0.267902926	0.662445	0	0	1.17768		0.05	0.0425	0.025	0
1	1.816490169	0.63	0.338565003	0.9053415	0	0	1.663473		0.033333333	0.028333333	0.025	0.024502915
1	2.062269312	0.865	0.412167313	1.251285	0	0	2.35536	0.147146341	0.044850205	0.038122674	0.025	0.052082758
1	2.156018696	1.018	0.467528413	1.4838768	0	0	2.8205436	0.209767442	0.063937116	0.054346549	0.03	0.066252073
1	2.752351331	1.15	0.414191309	1.678194	0	0	3.209178	0.242463415	0.073902849	0.062817421	0.03	0.076859289
1	3.343821293	1.275	0.378309691	1.8622065	0	0	3.577203	0.339808511	0.103573634	0.088037589	0.03	0.085836318
1.294255917	2.61903216	1.155103856	0.567003347	2.1860685	2.1	0.207348206	4.224927	0.42677551	0.130081176	0.110568999	0.03	0.09968498
1.372734924	2.987617709	1.322178061	0.604160296	2.6571405	2.4	0.144616783	5.167071	0.368813953	0.112414493	0.095552319	0.03	0.116559436
1.550820526	2.42343826	1.189692791	0.757188673	2.7013035	3	0.130189351	5.255397	0.462222222	0.140885333	0.119752533	0.03	0.117985697
1.70819123	2.644042673	1.03325668	0.665647351	2.590896	2.2	0.086381789	5.034582	0.376928571	0.114887829	0.097654654	0.035	0.11412911
1.881497632	2.178261773	0.989371428	0.851596453	2.7307455	2.1	0.078736402	5.314281	0.405477273	0.123589473	0.105051052	0.0335	0.118760287
2.33979309	2.313113687	0.771435734	0.778171869	2.64978	2.305505242	0.048015677	5.15235	0.3333125	0.10159365	0.086354603	0.035	0.116078771
2.577282472	2.059986707	0.653789415	0.815539243	2.473128	2.092123275	0.045739734	4.799046	0.353666667	0.1077976	0.09162796	0.035	0.110093604
4.186220123	1.809795226	0.383400766	0.88407792	2.35536	0.632839204	0.025156296	4.56351	0.294454545	0.089749745	0.076287284	0.035	0.105861767
4.550185903	1.85686322	0.323063723	0.791657665	2.163987	0.36104224	0.019001112	4.180764	0.23587234	0.071893889	0.061109806	0.04	0.098217829
3.80265861	2.471956587	0.349755299	0.538035339	1.957893	0.464581057	0.021554142	3.768576	0.23587234	0.071893889	0.061109806	0.04	0.089510568
3.092211166	1.804884543	0.349588027	0.598930278	1.5913401	1.258331848	0.035472973	3.0354702		0.1	0.085	0.04	0.071476129
2.269448125	1.880541243	0.414197615	0.502514903	1.3911345	0.815561261	0.028558033	2.635059		0.058823529	0.05	0.045	0.05931684
1.517479399	1.523193504	0.596383714	0.597429019	1.339611	0.8	0.05574555	2.532012		0.058823529	0.05	0.045	0.056015631
1.139356413	1.694055681	0.702150785	0.478142489	1.192401	0.7	0.10779152	2.237592		0.038461538	0.032692308	0.05	0.045286511
1.451135199	1.446724754	0.530619063	0.539148859	1.148238	0.55	0.047247956	2.149266		0.045454545	0.038636364	0.05	0.041961266
1.734573458	1.443900518	0.478503805	0.581757531	1.236564	0.494519777	0.022237801	2.325918		0.03125	0.0265625	0.05	0.048489327
1.705159313	1.604330973	0.448638432	0.486183969	1.148238	0.545508702	0.023356128	2.149266		0.032258065	0.027419355	0.055	0.041394488
1.5809977	1.785749137	0.502847031	0.453591147	1.192401	1.128853231	0.033598411	2.237592		0.04	0.034	0.055	0.044741055
1.564620795	2.511637997	0.47295805	0.302591377	1.118796	1.782001032	0.042213754	2.090382		0.05	0.0425	0.06	0.038503857
1	1	0.66	0.68	1.001028	0.5	1.031851136	1.854846		0.076923077	0.065384615	0.06	0.028550156
1	1	0.7	0.66	0.971586	0	0	1.795962		0	0		0.03366928
1	1	0.58	0.54	0.794934	0	0	1.442658		0	0		0.017308736
1	1	0.5	0.46	0.677166	0	0	1.207122		0	0		0.004396195
1	1	0.39	0.35	0.515235	0	0	0.88326		0	0		0
1	1	0.28	0.24	0.353304	0	0	0.559398		0	0		0
1	1	0.18	0.14	0.206094	0	0	0.264978		0	0		0
1	1	0.2	0.16	0.235536	0	0	0.323862		0	0		0
		0.631426694	0.504001971									

Rouse calculations not included in main text:

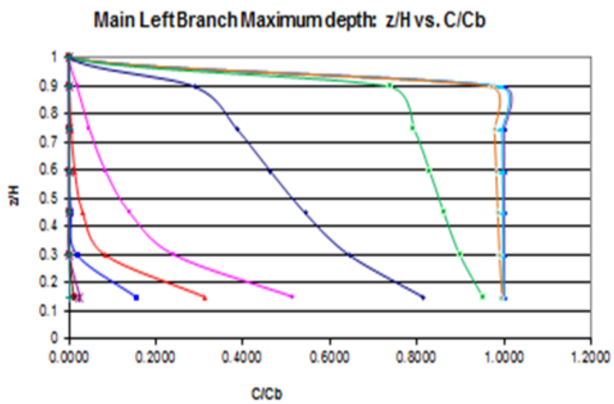

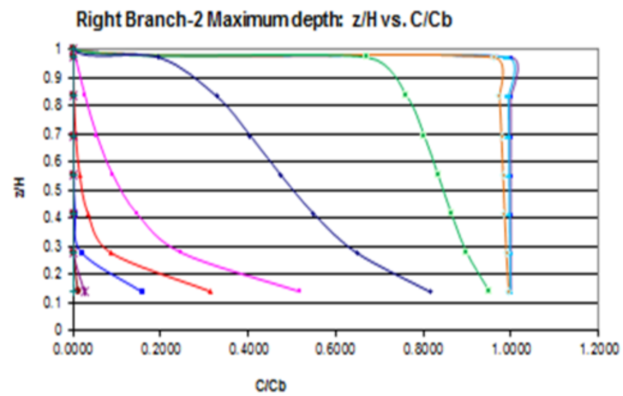

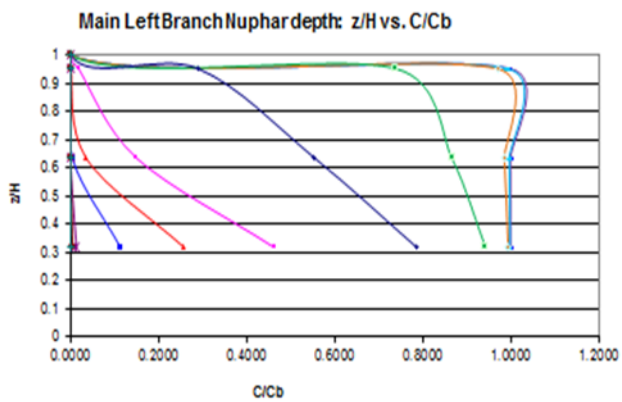

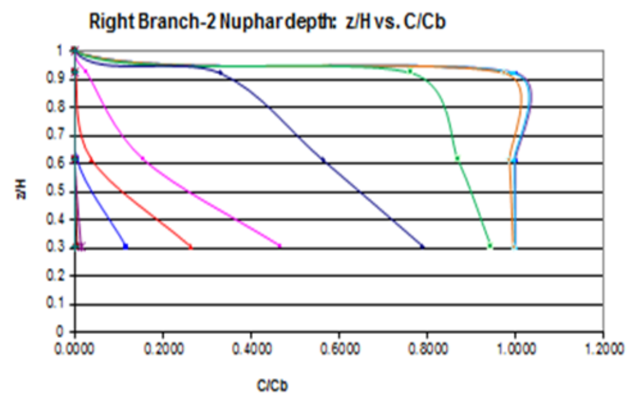

Core Data:

352 meters									
sample	depth	bulk density		% organic matter	C:N ratio	N elemental comp	15 N comp	C elemental comp	13 C comp
1	2.5	0.468405216	16.27454613	0.162745461	11.8877119	0.631472021	5.949285239	7.506757429	-28.79807474
2	5	0.90663992	13.47785108	0.134778511	9.6568407	0.659005159	5.338567982	6.363907844	-28.4279728
3	7.5	1.316369107	10.27783807	0.102778381	10.4744023	0.452331959	5.42149782	4.737906903	-28.04892674
4	10	1.533771314	9.719401883	0.097194019	13.07295	0.406674134	3.959673862	5.316430611	-28.51936336
5	12.5	1.435817452	9.285644099	0.092856441	9.63738873	0.389547651	3.587075632	3.754222139	-28.21818081
6	15	1.611524574	8.979779412	0.089797794	12.0840402	0.379450012	4.283318828	4.585289198	-28.32076676
7	17.5	1.552818455	9.373007439	0.093730074	15.9698412	0.326602185	3.340075944	5.215785021	-27.89056023
8	20	1.347522568	9.594859508	0.095948595	10.5490708	0.443123349	4.968267133	4.674539599	-27.77584305
9	22.5	1.562948847	10.04917881	0.100491788	10.5976035	0.438017894	4.886380162	4.641939967	-27.7833503
10	25	1.610411234	10.25888925	0.102588892	9.62614376	0.478481033	4.754582441	4.605927209	-28.38999793
11	27.5	1.681715145	10.08896275	0.100889628	9.87682287	0.403486818	5.640301531	3.985167835	-27.96727131
12	30	1.931203611	9.191838368	0.091918384	12.1861183	0.389593976	4.977513847	4.747638296	-27.79294778
13	32.5	1.744934804	9.209660746	0.092096607	12.10459	0.346277749	4.026560229	4.191550187	-28.32627273
14	35	1.913801404	7.243848696	0.072438487	12.4054287	0.284285141	3.668411082	3.526679047	-27.82565864
15	37.5	1.897121364	7.322194832	0.073221948	13.0948051	0.292868347	3.676020077	3.835053934	-27.65370919
16	40	1.715225677	8.849557522	0.088495575	16.4007543	0.337226289	4.552074396	5.530765517	-27.32809091
17	42.5	1.529839519	9.762704518	0.097627045	13.3434245	0.399991084	4.170369942	5.337250823	-28.80198756
18	45	1.25557673	9.675732218	0.096757322	13.2570581	0.420349573	4.153753206	5.572598708	-27.48541142
19	47.5	1.028194584	9.123451124	0.091234511	10.938729	0.394358846	3.667368268	4.313784551	-27.96293859
20	50	0.768465396	9.636563877	0.096365639	11.6296452	0.410601204	3.319719043	4.775146321	-28.00134242

800 meters								
sample	depth	bulk density	% organic matter	C:N ratio	N elemental comp	15 N comp	C elemental comp	13 C comp
1	2.5	0.284834504	34.40838742	10.8512887	1.399747943	6.9	15.18906906	-29.31580072
2	5	0.43332999	35.34637652	12.2287375	1.295447333	5.6	15.84168534	-29.32489041
3	7.5	0.457673019	32.34	11.9518141	1.224702129	5.44	14.63741212	-29.49797665
4	10	0.471023069	34.56703911	11.5612755	1.198859204	5.38	13.86034158	-29.12848784
5	12.5	0.411715145	34.99197432	11.8502668	1.282503355	5.34	15.19800692	-29.17427007
6	15	0.323229689	40.08797361	12.5829495	1.395377165	4.99	17.55796038	-29.06650818
7	17.5	0.369769308	36.94	12.1114538	1.262708745	4.94	15.29323857	-28.53282433
8	20	0.453881645	35.80864692	12.8729356	1.19494854	5.44	15.38249557	-29.28641146
9	22.5	0.429297894	34.19969895	12.4926603	1.212971708	5.99	15.15324354	-29.36458941
10	25	0.464062187	35.35757091	12.4798416	1.180642296	5.78	14.73422888	-29.08178107
11	27.5	0.499047141	37.15733015	11.3390317	1.326110176	7.32	15.03680531	-29.08149296
12	30	0.475937813	35.38461538	12.4179361	1.148830929	5.93	14.26610906	-29.34703217
13	32.5	0.427893681	39.06838454	11.6951589	1.167825717	5.74	13.65790729	-29.2226889
14	35	0.365125376	52.86554371	16.2476358	1.354230269	4.55	22.00304023	-28.20292765
15	37.5	0.440732197	48.78851331	18.9780379	1.190490801	4.87	22.59317949	-28.07372258
16	40	0.831003009	26.42978341	17.5699316	0.949667863	3.44	16.68559943	-28.46649758
17	42.5	0.931354062	21.85423897	15.2363271	0.780048173	2.99	11.88506908	-28.26144022
18	45	1.024974925	15.52137435	11.1002446	0.606169158	3.73	6.728625953	-28.03688639
19	47.5	0.483711133	13.6350015	12.4746297	0.528342696	3.97	6.590879473	-27.88966337
20	50	0.115897693	23.56465302	13.0250945	0.767609294	3.39	9.998183612	-28.15651001

548 meters				
sample	depth	bulk density	% organic matter by mass	
1	2.5	0.496980943	0.217137097	21.7137097
2	5	1.005877633	0.131714971	13.1714971
3	7.5	1.151775326	0.129375323	12.9375323
4	10	1.393560682	0.125536481	12.5536481
5	12.5	1.447703109	0.125035096	12.5035096
6	15	1.570782347	0.128971572	12.8971572
7	17.5	1.328565697	0.128975091	12.8975091
8	20	1.717141424	0.113432532	11.3432532
9	22.5	1.589919759	0.112933814	11.2933814
10	25	1.512557673	0.110387824	11.0387824
11	27.5	1.644132397	0.11222664	11.222664
12	30	1.690742227	0.098994007	9.89940068
13	32.5	1.543239719	0.129979645	12.9979645
14	35	1.296910732	0.14296499	14.296499
15	37.5	1.390601805	0.149570983	14.9570983
16	40	1.309227683	0.156279157	15.6279157
17	42.5	1.204322969	0.151779164	15.1779164
18	45	1.319819458	0.158028407	15.8028407
19	47.5	1.213430291	0.160131332	16.0131332
20	50	0.878004012	0.154110598	15.4110598

625 meters		
sample	depth	bulk density
1	2.5	0.547321966
2	5	0.589388164
3	7.5	0.583059178
4	10	0.352868606
5	12.5	0.69442327
6	15	0.730341023
7	17.5	0.71109328
8	20	0.697873621
9	22.5	0.705205617
10	25	0.744192578
11	27.5	0.705877633
12	30	0.729117352
13	32.5	0.877602808
14	35	0.809749248
15	37.5	0.636870612
16	40	0.713069208
17	42.5	0.857652959
18	45	0.765085256
19	47.5	0.736419258

Fowler (2014)'s CORE DATA								
		Inlet data: Lower Nuphar Marsh				Depth	BD, g/cc	% OM
Depth	%C	%N	C:N	d13 C	d15N	0	0.28	27.6
0	22.75	1.37	16.60584	-29.84	7.78	5	0.39	19.73
5	18.75	1.14	16.44737	-29.27	7.66	10	0.87	16.39
						15	1.22	14.74
10	18.63	1.04	17.91346	-28.22	6.97	20	1.47	10.3
						25	1.22	8.5
15					6.12	30	1.55	6.58
						35	1.52	8.73
20	15.15	0.58	26.12069	-27.51	4.56	40	1.3	
						45	1.29	
25						50	1.34	
30	8.28	0.47		-27.43	4.4			
35	9.34	0.52	17.96154	-27.74	4.24			
40	4.32	0.35	12.34286	-27.95	2.89			
45								
50								